

***CDKN2C*-Null Leiomyosarcoma: A Novel, Genomically Distinct Class of *TP53/RB1*-Wild-Type Tumor With Frequent *CIC* Genomic Alterations and 1p/19q-Codeletion**

Erik A. Williams, MD¹; Radwa Sharaf, PhD¹; Brennan Decker, MD, PhD²; Adrienne J. Werth, MD³; Helen Toma, MD³; Meagan Montesion, PhD¹; Ethan S. Sokol, PhD¹; Dean C. Pavlick, BS¹; Nikunj Shah, BS¹; Kevin Jon Williams, MD⁴; Jeffrey M. Venstrom, MD¹; Brian M. Alexander, MD, MPH¹; Jeffrey S. Ross, MD^{1,5}; Lee A. Albacker, PhD¹; Douglas I. Lin, MD, PhD¹; Shakti H. Ramkissoon, MD, PhD^{1,6}; and Julia A. Elvin, MD, PhD¹

PURPOSE Leiomyosarcoma (LMS) harbors frequent mutations in *TP53* and *RB1* but few actionable genomic alterations. Here, we searched for recurrent actionable genomic alterations in LMS that occur in the absence of common untreatable oncogenic drivers.

METHODS Tissues from 276,645 unique advanced cancers, including 2,570 uterine and soft tissue LMS, were sequenced by hybrid-capture–based next-generation DNA and RNA sequencing/comprehensive genomic profiling of up to 406 genes. We characterized clinicopathologic features of relevant patient cases.

RESULTS Overall, 77 LMS exhibited homozygous copy loss of *CDKN2C* at chromosome 1p32.3 (3.0% of LMS). Genomic alterations (GAs) in *TP53*, *RB1*, and *ATRAX* were rare compared with the remainder of the LMS cohort (11.7% v 73.4%, 0% v 54.5%, 2.6% v 24.5%, respectively; all $P < .0001$). *CDKN2C*-null LMS patient cases were significantly enriched for GAs in *CIC* (40.3% v 1.4%) at 19q13.2, *CDKN2A* (46.8% v 7.0%), and *RAD51B* (16.9% v 1.7%; all $P < .0001$). Chromosome arm-level aneuploidy analysis of available LMS patient cases ($n = 1,284$) found that 81% (58 of 72) of *CDKN2C*-null LMS exhibited 1p/19q-codeletion, a significant enrichment compared with 5.1% in the remainder of the LMS cohort ($P < .0001$). In total, 99% of *CDKN2C*-null LMS were in women; the median age was 61 years at surgery (range, 36-81 years). Fifty-five patient cases were uterine primary, four were nonuterine, and the remaining 18 were of uncertain primary site. Sixty percent of cases showed at least focal epithelioid variant histology. Most patients had advanced-stage disease, with 62% of confirmed uterine primary LMS at International Federation of Gynecology and Obstetrics stage IVB. We further validated our findings in two publicly available datasets: The Cancer Genome Atlas and the Project GENIE initiative.

CONCLUSION *CDKN2C*-null LMS defines a genomically distinct tumor that may have prognostic and/or therapeutic clinical implications, including possible use of specific cyclin-dependent kinase inhibitors.

JCO Precis Oncol 4:955-971. © 2020 by American Society of Clinical Oncology

Creative Commons Attribution Non-Commercial No Derivatives 4.0 License 

ASSOCIATED CONTENT

Appendix

Author affiliations and support information (if applicable) appear at the end of this article.

Accepted on April 24, 2020 and published at ascopubs.org/journal/po on September 1, 2020; DOI <https://doi.org/10.1200/P0.20.00040>

INTRODUCTION

Leiomyosarcoma (LMS), a neoplasm defined by smooth muscle differentiation, is the most common form of uterine sarcoma.¹ LMS is aggressive and resists standard therapy, with high rates of recurrence and progression. Multiple studies have shown an overall 5-year survival of 25%-76%, with survival for patients with metastatic disease at presentation approaching 10%-15%.² Stage of disease, as defined by the International Federation of Gynecology and Obstetrics (FIGO)³ or the American Joint Committee on Cancer (AJCC),⁴ at the time of diagnosis, is the most important prognostic factor for uterine LMS.¹ Surgery is the standard of care for

localized tumors, with hormonal and cytotoxic chemotherapy reserved for advanced stages.⁵

Genomic studies of LMS have demonstrated notable mutational heterogeneity, frequent inactivation of *TP53* and *RB1* through varied mechanisms, and widespread copy number alterations.⁶ LMS is often associated with complex karyotypes with numerous chromosomal gains and losses.⁷ LMS has demonstrated occasional potentially targetable genomic alterations (GAs), but novel targeted therapeutic agents have not been widely used.⁸⁻¹⁰ Herein, we describe a novel recurrent genomic signature of cyclin-dependent kinase inhibitor-2C gene (*CDKN2C*) homozygous loss in LMS primarily

CONTEXT

Key Objective

Leiomyosarcoma (LMS), an aggressive tumor with limited curative options, shows frequent mutations in *TP53* and *RB1* but few actionable genomic alterations. Here, we searched for recurrent actionable genetic alterations in LMS.

Knowledge Generated

A novel, genomically distinct class of LMS (3.0%; 77 of 2,570 cases) harbor homozygous loss of *CDKN2C*, which encodes the cyclin-dependent kinase inhibitor-2C. *CDKN2C*-null LMS lack typical *TP53* and *RB1* mutations; show concurrent homozygous deletion of *CIC*, *CDKN2A*, and *RAD51B*; and show frequent 1p/19q-codeletion.

Relevance

The finding of recurrent *CDKN2C*-null LMS provides insight into tumor biology and raises the possibility for use of specific cyclin-dependent kinase inhibitors in this aggressive disease.

from the uterus, with significantly low frequency of *TP53* and *RB1* GAs.

METHODS

Cohort and Genomic Analyses

Comprehensive genomic profiling was performed in a Clinical Laboratory Improvement Amendments–certified, College of American Pathologists–accredited laboratory (Foundation Medicine, Cambridge, MA). Approval for this study, including a waiver of informed consent and a HIPAA waiver of authorization, was obtained from the Western Institutional Review Board (Protocol No. 20152817). The pathologic diagnosis of each patient case was confirmed on routine hematoxylin and eosin (H&E)–stained slides. Sections were macrodissected to achieve > 20% estimated percent tumor nuclei in each case, for which the percent tumor nuclei equals 100 times the number of tumor cells divided by total number of nucleated cells. In brief, ≥ 60 ng of DNA was extracted from 40- μ m sections of tumor samples in formalin-fixed, paraffin-embedded tissue blocks. The samples were assayed by adaptor ligation hybrid capture, performed for all coding exons of 236 (v1), 315 (v2), or 405 (v3) cancer-related genes plus select introns from 19 (v1), 28 (v2), or 31 (v3) genes frequently rearranged in cancer (Appendix Table A1).^{11,12} For samples with available RNA, targeted RNA sequencing was performed for rearrangement analysis in 265 genes.¹² Sequencing of captured libraries was performed using the Illumina HiSeq 4000 System (Illumina, San Diego, CA) to a mean exon coverage depth of targeted regions of > 500 \times , and sequences were analyzed for GAs, including short variant alterations (base substitutions, insertions, and deletions), copy number alterations (focal amplifications and homozygous deletions), and select gene fusions or rearrangements.^{11,13,14} To maximize mutation detection accuracy (sensitivity and specificity) in impure clinical specimens, the test was previously optimized and validated to detect base substitutions at a $\geq 5\%$ mutant allele frequency, indels with a $\geq 10\%$ mutant allele frequency with \geq

99% accuracy, and fusions occurring within baited introns/exons with > 99% sensitivity.¹¹ Germline and somatic status of pathogenic alterations was not delineated. Tumor mutational burden (TMB; mutations/Mb) was determined on 0.8-1.1 Mb of sequenced DNA.¹⁴ Microsatellite instability was determined on up to 114 loci.¹⁵

Copy number analysis. Copy number analysis to detect gene-level amplifications at > 6-8 copies depending on tumor ploidy and homozygous deletions was performed as previously described.¹¹ In brief, the aligned DNA sequences of each tumor specimen were normalized against a process-matched normal, producing log-ratio and minor allele frequency data. Next, whole-genome segmentation was performed using a circular binary segmentation algorithm on the log-ratio data. A Gibbs sampler fitted copy number model and a grid-based model were fitted to the segmented log-ratio and minor allele frequency data, producing genome-wide copy number estimates. Finally, the degrees-of-fit of candidate models returned by Gibbs sampling and grid sampling were compared, and the optimal model was selected by an automated heuristic.

Signal-to-noise ratios for each genomic segment were used to determine gain or loss per chromosome arm on the basis of tumor purity and ploidy; the sum of segment sizes determined the fraction of each arm gained or lost. Chromosomes were assessed for arm-level aneuploidy, defined as positive if > 50% of the arm was altered. This threshold was previously validated on 109 *IDH1/2*-mutant glioma samples with 1p/19q-codeletion fluorescence in situ hybridization (FISH) results available. Patient cases were blinded to FISH results, and 1p/19q-codeletion status was determined via arm-level aneuploidy analysis. Concordance was 95%, sensitivity was 91%, and positive predictive value was 100%. A query for chromosome 1p and 19q arm-level aneuploidy was performed on LMS patient cases with available aneuploidy data (n = 1,284), with positive patient cases defined as 1p/19q-codeleted.

Clinicopathologic analysis of LMS cohort harboring homozygous CDKN2C deletion. The cohort of CDKN2C-null LMS comprised 77 cases, each from a different patient, that were submitted to Foundation Medicine for comprehensive genomic profiling during routine clinical care. Human investigations were performed after approval by a local human investigations committee and in accordance with an assurance filed with and approved by the Department of Health and Human Services, when appropriate. Clinicopathologic data, including patient age, sex, tumor site, and FIGO stage or AJCC (8th edition) stage, were extracted from the accompanying pathology report.^{4,16} Primary site data were not available for a subset of patient cases (“indeterminant primary”). The histopathology was assessed on routine H&E-stained slides of tissue sections submitted for genomic profiling by two board-certified pathologists (E.A.W., D.I.L.).

Quantitative data were analyzed using the Fisher exact test because of the categorical quality of the data and the size of the cohort. For the age and TMB comparisons between two groups, the nonparametric Mann-Whitney *U* test was used. A two-tailed *P* value of < .05 was considered statistically significant; the Bonferroni correction was applied for multiple simultaneous comparisons.

Review of publicly available datasets. The Cancer Genome Atlas (TCGA) Network’s sarcoma genomic dataset¹⁷ and the American Association for Cancer Research (AACR) Project GENIE Consortium dataset (v7.0-public)¹⁸ were interrogated for LMS with homozygous loss of CDKN2C. Histopathology of TCGA patient cases was reviewed by two board-certified pathologists (E.A.W., D.I.L.).

RESULTS

A Novel Class of CDKN2C-Null LMS: Clinicopathologic Features

From an internal series of 276,645 unique advanced cancers, including 2,570 LMS, of which 939 were of confirmed uterine origin, we identified 77 LMS with homozygous copy loss of CDKN2C at chromosome 1p32.3 (3.0% of all LMS [77 of 2,570], 5.9% of uterine LMS [55 of 939]). Clinical characteristics of the 77 patients with this novel class of CDKN2C-null LMS are summarized in Table 1. These patients were significantly older than the remainder of the LMS cohort (median age, 61 v 57 years; *P* = .0009, Mann-Whitney *U* test). Patients were enriched for female sex compared with the remainder of the LMS cohort (99% [76 of 77] v 79% [1,968 of 2,493]; *P* < .0001, Fisher’s exact test). Six female patients had a prior history of leiomyomatosis (*n* = 2) or uterine smooth muscle tumor of uncertain malignant potential (STUMP; *n* = 4). The majority of CDKN2C-null LMS patients showed clinically advanced/metastatic disease, with 62% of confirmed uterine primary occurrences documented at FIGO stage IV (*n* = 34 of 55) and 86% of indeterminant or soft tissue primary cases documented at AJCC stage IV (*n* = 19/22), as summarized

TABLE 1. Clinical Characteristics of Patients With CDKN2C-Null Leiomyosarcoma

Characteristic	No. (%)
No. of patients	77
Median (range) age at diagnosis, years	61 (36-81)
Sex	
Female	76 (99)
Male	1 (1)
Primary site	
Uterine	55 (71)
Soft tissue	4 (5)
Indeterminant	18 (23)
FIGO staging (uterine primary)	
IB	6 (11)
IIA	2 (4)
IIB	4 (7)
IIIA	2 (4)
IIIB	1 (2)
IIIC	4 (7)
IVB	34 (62)
Unknown	3 (6)
AJCC staging (soft tissue or indeterminant primary)	
IA	1 (5)
IV	19 (86)
Unknown	2 (9)

Abbreviations: AJCC, American Joint Committee on Cancer; FIGO, International Federation of Gynecology and Obstetrics.

in Table 1. Locations of the sequenced tumor specimens are summarized in Appendix Table A2.

Comprehensive Genomic Profiling of CDKN2C-Null LMS

The distribution of GAs in the 77 CDKN2C-null LMS is displayed in Figure 1. TP53, RB1, and ATRX GAs were rare in comparison with the remainder of the LMS cohort (Table 2; Appendix Table A3). CDKN2C-null LMS comprised 14% (68 of 486) of TP53/RB1–wild-type LMS. The most frequent GAs were identified in C1C at 19q13.2, CDKN2A, and RAD51B (Table 2), and unsupervised analysis showed significant enrichment of these alterations in the CDKN2C-null cohort (Appendix Fig A1). Eighty-five percent (60 of 71) of patient cases evaluated for FAF1 showed homozygous deletion of FAF1 at 1p32.3, a gene adjacent to CDKN2C (9.7 kb apart). No CDKN2C-null LMS in our cohort had inactivating GAs in FUBP1 or pathogenic alterations in IDH1/2 or TERTp.

The median TMB was 2.4 mutations/Mb (range, < 0.8-9.6; Q1-Q3, 1.6-3.2), similar to the remainder of the LMS cohort (median, 2.4 mutations/Mb; range, < 0.8-203; Q1-Q3, 1.6-4.0) but slightly lower overall (*P* = .0425, Mann-Whitney

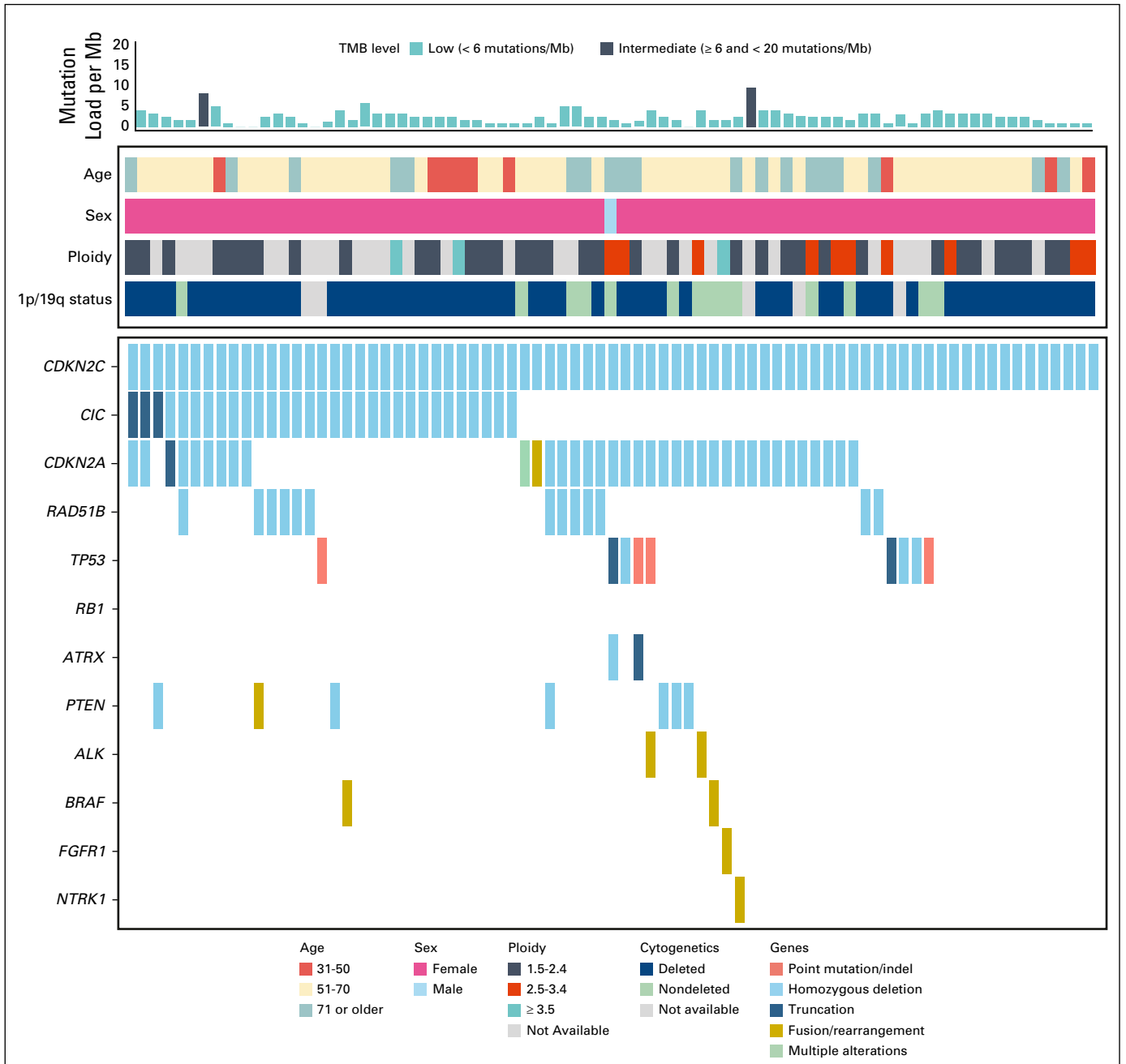


FIG 1. Mutational landscape of *CDKN2C*-null leiomyosarcoma. Summary tile plot of pathogenic variants identified in 77 cases of *CDKN2C*-null leiomyosarcoma. Each column represents data for a single patient. Age, sex, tumor ploidy, and 1p/19q-codeletion status are also provided for each case. The histogram on top shows tumor mutational burden (TMB; mutations/megabase).

U test). No microsatellite-unstable patient cases were present in the *CDKN2C*-null cohort.

Within the cohort of *CDKN2C*-null LMS, comparison of patients < 61 years of age with patients ≥ 61 years revealed significant differences in frequency of *CIC* alterations (54% [20 of 37] v 28% [11 of 40]; $P = .022$) and *RAD51B* alterations (5% [2 of 37] v 28% [11 of 40]; $P = .0136$). No other significant differences based on age were identified. Comparison of patient cases on the basis of clinical stage,

history of lower grade smooth muscle neoplasm, or primary site did not reveal any significant differences in GAs.

Three patients had two separate tissue specimens analyzed (Appendix Table A4). For all three patients, each initial sequencing result, including *CDKN2C* loss, was identified in the subsequent paired-specimen result. One patient had sequencing of both the primary uterine LMS and a subsequent lung metastasis. The lung mass showed additional homozygous loss of *CIC*.

TABLE 2. Comparative Demographics and Percent Frequency of Genomic Alterations Stratified by CDKN2C Status

Variable	CDKN2C-Null LMS	Remaining LMS Cohort	P
Female sex, % (n/total N)	99 (76/77)	79 (1,968/2,493)	< .0001
Median (range) age, years	61 (36-81)	57 (< 1 to > 89)	.0009
TMB (Q1–Q3), mut/Mb, % (n/total N)	2.4 (1.6-3.2)	2.4 (1.6-4.0)	.0425
MSI high, % (n/total N)	0 (0/63)	0.2 (5/2,093)	1.0000
Genomic alteration, % (n/total N)			
1p/19q-codeletion	85 (33/39)	5 (62/1,212)	< .0001
CIC	40 (31/77)	1 (35/2,473)	< .0001
CDKN2A	47 (36/77)	7 (175/2,493)	< .0001
RAD51B	17 (13/77)	2 (43/2,473)	< .0001
TP53	12 (9/77)	73 (1,830/2,493)	< .0001
RB1	0 (0/77)	55 (1,359/2,493)	< .0001
ATRX	3 (2/77)	25 (606/2,473)	< .0001
PTEN	9 (7/77)	16 (399/2,493)	.113
ALK fusion	3 (2/77)	2 (41/2,493)	.371
BRAF fusion	3 (2/77)	0.2 (4/2,493)	.0123
FGFR1 fusion	1 (1/77)	0.1 (2/2,493)	.0873
NTRK1 fusion	1 (1/77)	0.1 (3/2,493)	.115

NOTE. For percent values, number of positive cases over the total number of evaluated cases is included in parentheses. The Bonferroni correction for 16 simultaneous comparisons was applied; significant P values (< .003) are in bold.

Abbreviations: LMS, leiomyosarcoma; MSI, microsatellite instability; TMB, tumor mutational burden.

A query and review for chromosome 1p and 19q arm-level aneuploidy in available LMS patient cases (n = 1,284) revealed that 99% (71 of 72) of CDKN2C-null LMS patient cases had whole-arm aneuploidy of the short arm of chromosome 1, and 81% (58 of 72) had aneuploidy of the long arm of chromosome 19 and 1p/19q-codeletion. Significant enrichment for 1p/19q-codeletion was identified in comparison with the remainder of the evaluated LMS cohort (81% [58 of 72] v 5% [62 of 1,212]; P < .0001). Copy number plots of two exemplary cases of CDKN2C-null LMS exhibiting 1p/19q-codeletion are shown in Figures 2A and 2B. Additional recurrent chromosomal arm-level changes were identified in the 72 patient cases available, including most frequently aneuploidy of chromosomes 6p (n = 35), 9p (n = 19), 10q (n = 28), 11p (n = 39), 13q (n = 46), 14q (n = 46), and 16q (n = 52).

A review of 1p/19q-codeletion status in available LMS patient cases without homozygous deletion of CDKN2C (n = 1,212) revealed 62 1p/19q-codeleted LMS (5%; Fig 2C). These 62 CDKN2C-retained LMS showed GAs in TP53 (52%; n = 33), RB1 (45%; n = 28), ATRX (16%; n = 10), and PTEN (13%; n = 8). GAs were also identified in CDKN2A (23%; n = 14) and ALK (10%; n = 6; all activating rearrangement events). A minority showed GAs in RAD51B (8%; n = 5), CIC (7%; n = 4; all homozygous loss), and FAF1 (5%; n = 3). Three of the four patient cases with homozygous deletion of CIC also showed homozygous deletion of both RAD51B and FAF1. All four occurred in uterine LMS (one of which with a history of STUMP).

All non-LMS sarcoma patient cases in the Foundation Medicine dataset (n = 12,097) were evaluated for CDKN2C status. Twenty-two of 1,297 gastrointestinal stromal tumors (GISTs) were CDKN2C-null (1.7% of GISTs). Twenty-one had a KIT mutation, and the single remaining GIST had a PDGFRA mutation. None of the 14 CDKN2C-null GIST cases with 1p/19q data had 1p/19q codeletion. Nineteen additional sarcoma occurrences with homozygous deletion of CDKN2C were identified (0.18% of non-LMS non-GIST sarcomas). These included diverse sarcoma diagnoses, including six high-grade sarcomas not otherwise specified, two osteosarcomas, two malignant peripheral nerve sheath tumors, and two inflammatory myofibroblastic tumors. Genomics were also varied, with alterations identified in CDKN2A (68%; n = 13), TP53 (42%; n = 8), NF1 (26%; n = 5), NF2 (26%; n = 5), and ALK (16%; n = 3; all activating rearrangement events). No GAs in CIC or RAD51B were identified. Eleven of the 19 patient cases had 1p/19q-codeletion data available; two (18%) of the 11 had 1p/19q-codeletion. Both were ALK rearrangement–positive tumors in women (ages, 63 and 72 years).

We also searched our entire LMS cohort (N = 2,570) for cases with pathogenic alterations in CDKN2C other than homozygous deletion. Only one case was identified, in a 52-year-old woman with an estrogen receptor–positive, progesterone receptor–positive (per report, by immunohistochemistry) uterine LMS with a truncating mutation in CDKN2C (p.R68*). Concurrent homozygous deletions of CIC

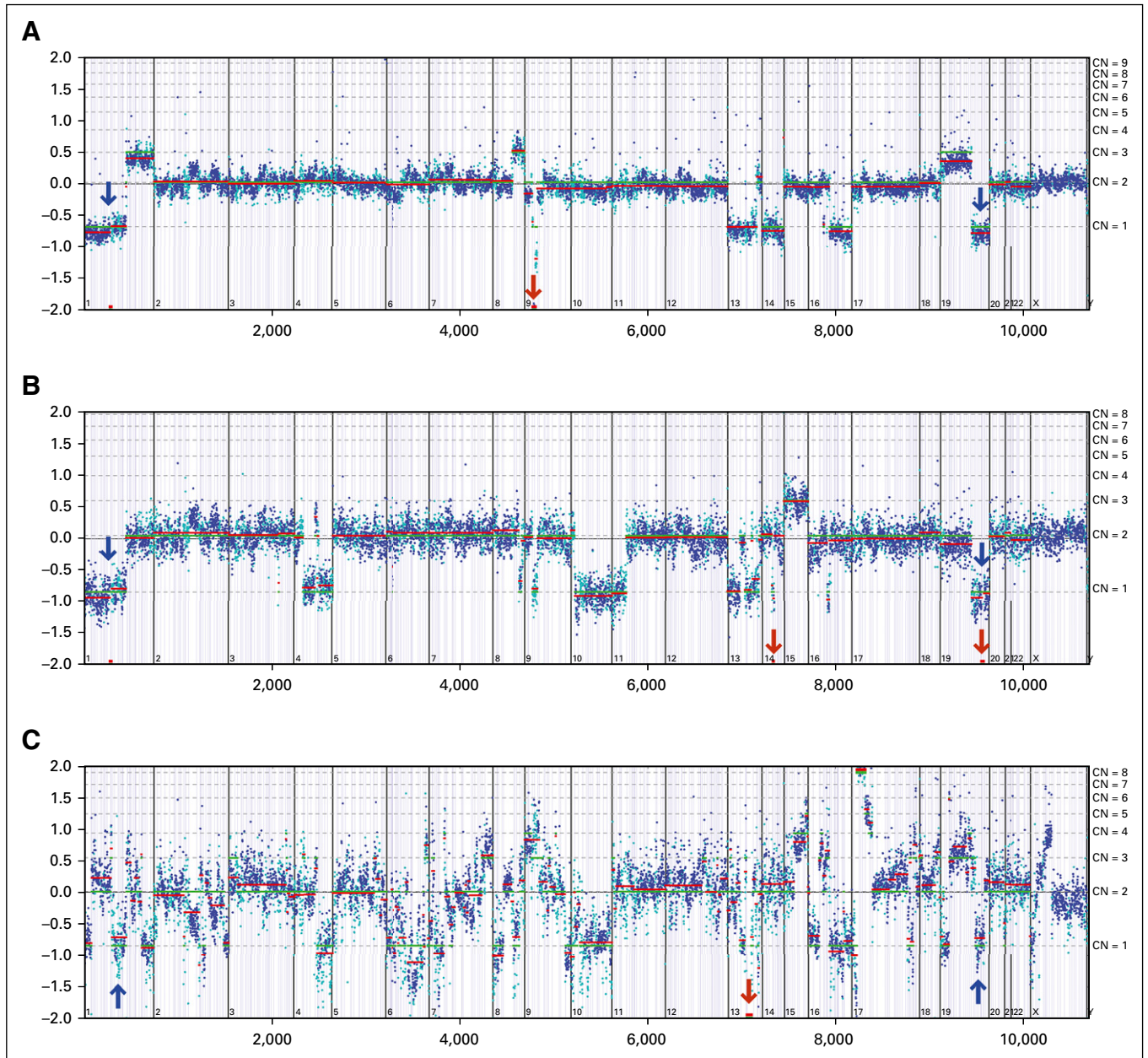


FIG 2. Copy number (CN) plots of three leiomyosarcomas (LMS) with known *CDKN2C* status and 1p/19q-codeletion (blue arrows). The y-axes display log-ratio measurements of coverage from each case as compared with a normal reference sample, with assessed CNs denoted by dashed horizontal lines. Each dot represents a genomic region evaluated by the assay (cyan, single-nucleotide polymorphism; blue, exon), which are organized by genomic position. Red lines designate average log-ratio in a segment, and green lines represent model prediction. (A) *CDKN2C*-null LMS with a truncating variant in *CIC* (p.Q907*) and homozygous deletion of *CDKN2A* at chromosome 9p21.3 (red arrow). (B) *CDKN2C*-null LMS with homozygous deletion of *CIC* at chromosome 19q13.2 (red arrow) and *RAD51B* at chromosome 14q24.1 (red arrow). (C) *CDKN2C*-retained LMS with deep deletion of *RB1* at chromosome 13q14.2 (red arrow) and a CN plot of high complexity.

and *RAD51B* were identified; 1p/19q status was not available.

Histopathology

Histopathologic evaluation was performed on all available high-resolution digital pathology H&E slides of our cohort of *CDKN2C*-null LMS (n = 70). Histology was heterogeneous, as shown in Figure 3. Twenty-seven cases (39%) were

epithelioid LMS. Twenty-three cases (33%) were spindle cell LMS. Nineteen cases (27%) showed mixed histology, including 11 mixed spindle and epithelioid LMS; four mixed spindle and myxoid LMS; two mixed epithelioid and myxoid LMS; and two mixed spindle, epithelioid, and myxoid LMS. A single case showed small round cell morphology.

Per immunohistochemistry reports, *CDKN2C*-null LMS showed diffuse positivity for estrogen receptor (29 of 29 LMS) and

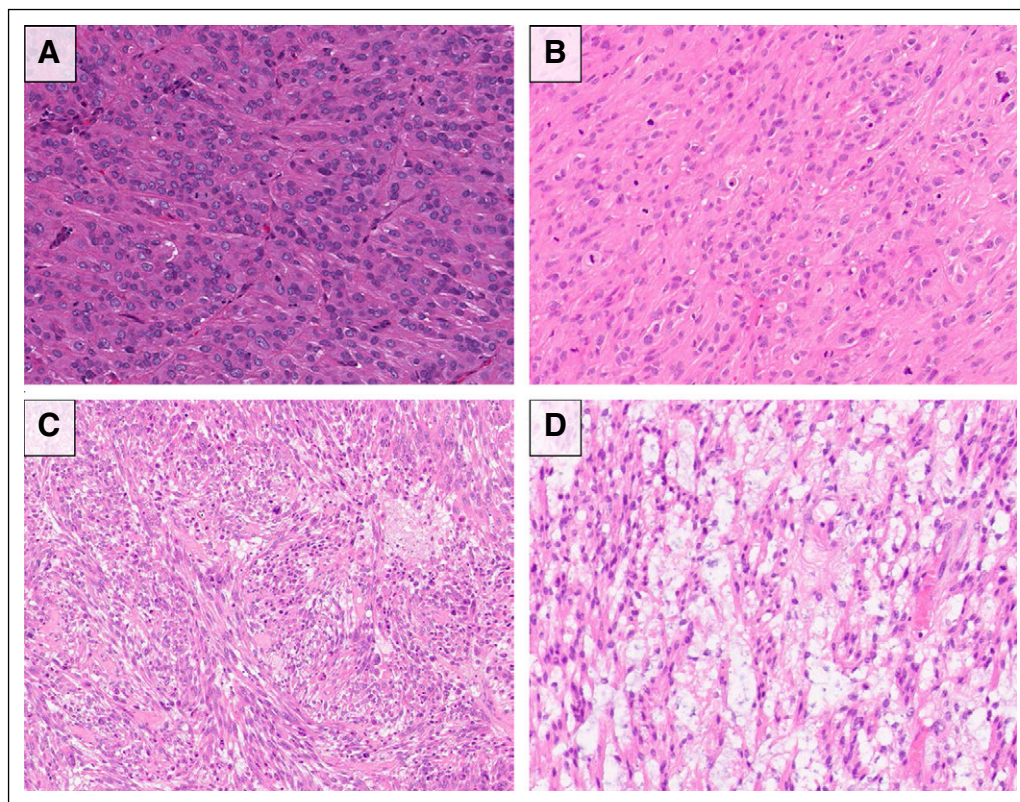


FIG 3. Histopathology of *CDKN2C*-null leiomyosarcoma ranged from (A, B) epithelioid to (C) spindle (hematoxylin & eosin [H&E] stains, 200 \times). (D) Occasional cases showed focal myxoid histology (H&E stain, 200 \times).

progesterone receptor (24 of 26; remaining two with focal positivity). *CDKN2C*-null LMS were also positive for desmin (30 of 33; remaining three with focal positivity), smooth muscle actin (25 of 25), muscle-specific actin (11 of 11), and caldesmon (6 of 6). HMB-45 was focally positive in two of nine cases, and CD10 was positive in one of 14 cases. Tumors were reportedly negative for S100 (n = 15), various keratin markers (n = 19), CD34 (n = 11), and CD117 (n = 11).

Publicly Available Datasets

The frequency of *CDKN2C*-null cases in LMS in our dataset prompted us to interrogate the sarcoma genomic dataset of TCGA Network¹⁷ and the AACR Project GENIE Consortium dataset (v7.0-public).¹⁸ A total of 12 *CDKN2C*-null LMS patient cases were identified (TCGA: n = 3 [4%] of 80; GENIE: n = 9 [2%] of 449; Table 3). The *CDKN2C*-null LMS patient cases were enriched for female sex (n = 12 of 12), uterine origin, and epithelioid histology. Patient cases showed frequent homozygous loss of *CIC* (n = 5 [42%] of 12), *CDKN2A* (n = 4 [33%] of 12), and *RAD51B* (n = 3 [25%] of 12), and all were wild type for *TP53*, *RB1*, and *ATRX* (n = 12 of 12).

DISCUSSION

In 2,570 patient cases of LMS, *CDKN2C*-null LMS (n = 77; 3.0%) comprised a genomically distinct molecular subgroup.

CDKN2C-null LMS typically lacked mutations in *TP53*, *RB1*, and *ATRX* but showed frequent 1p/19q-codeletion (81%), and nearly half (40.3%) showed homozygous deletion or inactivating truncations of *CIC*. Clinical features were significantly different from other LMS: patients were slightly but statistically significantly older, and the vast majority (76 of 77 patients) were women. Most were of uterine primary site of origin. A high percentage demonstrated epithelioid variant features on histology, and limited clinical data suggest a possible association with and progression from lower-grade uterine smooth tumors, such as leiomyomatosis and STUMP.

CDKN2C at 1p32.3 encodes the homologous p18INK4C cell cycle regulatory protein that blocks cell cycle progression by inhibiting the cyclin D-dependent kinases CDK4 and CDK6.¹⁹⁻²¹ Loss of *CDKN2C* results in loss of potent inhibition of CDK4/6 in the cyclin D-CDK4/6-INK4-Rb pathway. *CDKN2C* is also a key factor for ATM/ATR-mediated activation of the tumor suppressor p53, and *CDKN2C* loss has been shown to block p53 induction in response to DNA damage.^{22,23} *CDKN2C* loss has been documented in a subset of diverse tumor types, including multiple myeloma, pituitary adenoma, and thyroid carcinoma.²⁴⁻²⁶ *CDKN2C* loss has also been documented in a small percentage of oligodendroglioma.^{27,28} The adjacent *FAF1* gene at 1p32.3 encodes FAS-associated factor 1,

TABLE 3. CDKN2C-Null Leiomyosarcoma From Two Independent Cohorts

Sample	Age	Sex	Uterine	Additional Genomic Alterations	Histology	Disease Status	Survival Status
TCGA-K1-A42X	62	F	Yes	Homozygous loss of <i>CIC</i> and <i>RAD51B</i> ; amplification of <i>CCND1</i> and <i>FGF19</i>	Epithelioid and spindle	Local recurrence at 67 months	Living at 123 months
TCGA-FX-A3RE	65	F	Yes	Homozygous loss of <i>CIC</i> , <i>CDKN2A</i> , and <i>RAD51B</i> ; amplification of <i>MET</i> , <i>BRAF</i> , <i>EZH2</i> , and <i>RHEB</i>	Epithelioid and spindle	Disease free at 21 months	Living at 21 months
TCGA-1W-A3M6	59	F	Yes	Homozygous loss of <i>CDKN2A</i> and <i>KMT2C</i> ; amplification of <i>MDM4</i> , <i>NTRK1</i> , <i>ALK</i> , <i>IKBKE</i> , <i>AKT3</i> , <i>MCL1</i> , and <i>DDR2</i>	Epithelioid and spindle	Disease free at 22 months	Living at 22 months
GENIE-DFCI-024530	73	F	Yes	None	Epithelioid, per report	Not available	Not available
GENIE-DFCI-090524	79	F	Unknown	Homozygous loss of <i>CIC</i> ; <i>ARID1A</i> p.Q1095Afs*10; amplification of <i>ERBB2</i> and <i>PPM1D</i>	Not available	Not available	Not available
GENIE-DFCI-108895	66	F	Yes	Homozygous loss of <i>CDKN2A</i> and <i>CDKN1A</i>	Not available	Not available	Not available
GENIE-DFCI-118367	72	F	Unknown	Homozygous loss of <i>CHEK2</i>	Not available	Not available	Not available
GENIE-DFCI-118421	54	F	Yes	Homozygous loss of <i>CIC</i> , <i>P TEN</i> , and <i>FAS</i> ; <i>RNF43</i> p.L17Afs*24	Epithelioid, per report	Not available	Not available
GENIE-MSK-P-0028037	36	F	Yes	Homozygous loss of <i>BBC3</i> on 19q13.32	Not available	Not available	Not available
GENIE-MSK-P-0030528	60	F	Yes	<i>CIC-ERF</i> fusion	Not available	Not available	Not available
GENIE-MSK-P-0034923	44	F	Yes	Homozygous loss of <i>CIC</i> , <i>ERF</i> , <i>ERCC2</i> , and <i>BBC3</i> at 19q13; homozygous loss of <i>RAD51B</i> and <i>P TEN</i> ; <i>CIC</i> p.H505Pfs*9; <i>HOXB13</i> X201_splice	Not available	Not available	Not available
GENIE-VICC-439861	71	F	Unknown	Homozygous loss of <i>CDKN2A</i> ; amplification of <i>CCND1</i> and <i>FGF19</i> ; <i>CHEK2</i> p.K287Rfs*17	Not available	Not available	Not available

NOTE. TCGA rows were identified from The Cancer Genome Atlas,¹⁷ from a total of 80 leiomyosarcoma. GENIE rows were identified from project GENIE dataset,¹⁸ from a total of 449 leiomyosarcoma with copy number alteration data.

which enhances FAS-mediated apoptosis, and its loss may contribute to tumor pathogenesis.²⁹

The *CIC* gene on chromosome 19q13.2 represses genes induced downstream to RTK pathway activation.³⁰ In the absence of RTK signaling, *CIC* blocks transcription of genes that have diverse effects on cellular proliferation, metabolism, and migration.³¹ Along with single copy loss of *CIC* on 19q, concurrent inactivating mutations in *CIC* are identified in a high percentage of oligodendrogliomas.³²

Whole-arm 1p/19q-codeletion, with concurrent mutation in *IDH1* or *IDH2*, is entity-defining for oligodendrogliomas.³³⁻³⁵ Oligodendrogliomas are associated with relatively long overall survival, and treatment strategies are often stratified on the basis of 1p/19q status.³⁶⁻³⁸ The codeletion is a result of unbalanced translocation between two chromosomes, with subsequent loss of der(1;19)(p10;q10), likely because chromosomes 1 and 19 are near each other in the nonrandom organization of the nucleus.³⁹⁻⁴¹ A large percentage of oligodendrogliomas also show *CIC* and *FUBP1* mutations.³¹ Our cohort of *CDKN2C*-null LMS shows notable similarities and differences to oligodendroglioma; 40% of our cohort showed an inactivating alteration in *CIC*, most commonly homozygous deletion. Although *FUBP1* at 1p31.1 is somatically mutated in a subset of oligodendroglioma, no *CDKN2C*-null LMS patient cases in our cohort had inactivating GAs in *FUBP1* or pathogenic alterations in *IDH1/2* or *TERTp*. The recurrent chromosomal arm-level losses in our cohort may indicate that additional tumor suppressor genes are located on these arms. Rare sarcoma-like tumors originating from oligodendrogliomas have been reported, with documented *IDH1* mutation and 1p/19q-codeletion, and have been termed “oligosarcoma.”⁴²⁻⁴⁴ Rodriguez et al⁴³ identified 6 of 7 patient cases of oligosarcoma with at least focal smooth muscle actin positivity of the sarcomatous component by immunohistochemistry and one patient case with smooth muscle differentiation by electron microscopy. These results indicate a similarity in differentiation to our cohort of LMS.

Among all sarcomas with *CDKN2C* loss, 1p/19q-codeletion appears to be nearly exclusive to LMS. In our overall LMS cohort, however, occasional *CDKN2C*-retained LMS showed *TP53* and *RB1* alterations and were positive by the 1p/19q-codeletion detection algorithm. We speculate that, given the complexity of these genomically unstable occurrences, occasional *CDKN2C*-retained LMS satisfy these criteria (Fig 2C). As such, identification of homozygous deletion of *CDKN2C* may be the most specific distinguishing feature.

Cytogenetic findings in LMS and leiomyoma have been previously reported, although without characterization of *CDKN2C* status. A greater frequency of 1p loss has been

documented in metastasized LMS.⁴⁵ From a cytogenetics study of 800 uterine leiomyomata, nine diploid occurrences with 1p loss were identified, with other associated alterations, particularly chromosome 19 and/or chromosome 22 loss.⁴⁶ Transcriptional profiling of two of the 1p-deleted leiomyomas in that study showed alignment with malignant LMS in a hierarchical clustering analysis.⁴⁶ In another study, 1p loss was identified in approximately one quarter of uterine cellular leiomyomata.⁴⁷ Three reports on a total of eight pulmonary-based “benign metastasizing leiomyoma” reported 19q and 22q terminal deletion in each case.⁴⁸⁻⁵⁰ Rare uterine leiomyomas with GAs in *RAD51B* have also been identified.⁵¹ The overlap in GAs between our cohort of *CDKN2C*-null LMS and a subset of leiomyoma of uncertain *CDKN2C* status in the literature suggests a possible connection between these entities.

Evaluations of GAs in epithelioid or myxoid uterine smooth muscle neoplasms are limited in the literature.⁵²⁻⁵⁶ Although a high percentage of *CDKN2C*-null LMS in our study demonstrated epithelioid features on histology, histology was also varied. Immunohistochemistry results extracted from pathology reports were typical for uterine LMS, with expression of characteristic smooth muscle markers.⁵⁷

Given the overall low response rate of LMS to standard therapies, the identification of this targetable alteration in *CDKN2C* may be useful for treatment decisions. CDK4/6 inhibitors have previously shown effectiveness in a LMS with a *CDKN2A* alteration.¹⁰ Nearly half of the *CDKN2C*-null LMS harbored loss of *CDKN2A*; CDK4/6 inhibitors may be effective in replacing the loss of inhibition of CDK4/6 that results from *CDKN2C* and *CDKN2A* loss in these patient cases that recur after standard chemotherapy regimens. A minor subset of *CDKN2C*-null and/or 1p/19q-codeleted LMS harbored activating fusions in *ALK*, *BRAF*, *FGFR1*, and *NTRK1*, for which targeted inhibitors may be of utility.⁹

Limitations of this study include its retrospective nature and the enrichment for aggressive tumors, mostly metastatic to distant sites. The latter may be due to collection bias from submission of specimens later in the disease course.

Additional studies will be needed to correlate the finding of *CDKN2C* loss in LMS with prognostic data and treatment outcomes. If clinically indicated, future studies are needed to evaluate other diagnostic modalities, such as *CDKN2C* testing through immunohistochemical surrogates^{58,59} or 1p/19q FISH testing. Future studies are also needed to identify the gene expression profile of this novel genomic subtype.⁶⁰ Comprehensive genomic profiling of LMS may provide insights into LMS biology and potentially inform therapeutic options, including specific cyclin-dependent kinase inhibitors.

AFFILIATIONS

¹Foundation Medicine, Cambridge, MA

²Department of Pathology, Brigham and Women’s Hospital and Harvard Medical School, Boston, MA

³Christiana Hospital, Department of Obstetrics and Gynecology, Newark, DE

⁴Department of Physiology, Department of Medicine, Lewis Katz School of Medicine at Temple University, Philadelphia, PA

⁵Department of Pathology, State University of New York Upstate Medical University, Syracuse, NY

⁶Wake Forest Comprehensive Cancer Center and Department of Pathology, Wake Forest School of Medicine, Winston-Salem, NC

CORRESPONDING AUTHOR

Erik A. Williams, MD, 150 Second St, Cambridge, MA 02141; Twitter: @ErikAWilliamsM1; e-mail: erwilliams@foundationmedicine.com.

EQUAL CONTRIBUTION

D.I.L., S.H.R., and J.A.E. contributed equally to this work.

AUTHOR CONTRIBUTIONS

Conception and design: Erik A. Williams

Administrative support: Brian M. Alexander

Financial support: Brian M. Alexander

Collection and assembly of data: Erik A. Williams, Brennan Decker, Meagan Montesion, Dean C. Pavlick, Nikunj Shah, Jeffrey S. Ross, Lee A. Albacker, Douglas I. Lin, Shakti H. Ramkissoon

Data analysis and interpretation: Erik A. Williams, Radwa Sharaf, Brennan Decker, Adrienne J. Werth, Helen Toma, Meagan Montesion, Ethan S. Sokol, Dean C. Pavlick, Kevin Jon Williams, Jeffrey M. Venstrom, Brian M. Alexander, Jeffrey S. Ross, Lee A. Albacker, Douglas I. Lin, Shakti H. Ramkissoon, Julia A. Elvin

Manuscript writing: All authors

Final approval of manuscript: All authors

Accountable for all aspects of the work: All authors

AUTHORS' DISCLOSURES OF POTENTIAL CONFLICTS OF INTEREST

The following represents disclosure information provided by authors of this manuscript. All relationships are considered compensated unless otherwise noted. Relationships are self-held unless noted. I = Immediate Family Member, Inst = My Institution. Relationships may not relate to the subject matter of this manuscript. For more information about ASCO's conflict of interest policy, please refer to www.asco.org/rwc or ascopubs.org/po/authors/author-center.

Open Payments is a public database containing information reported by companies about payments made to US-licensed physicians (Open Payments).

Erik A. Williams

Employment: Foundation Medicine, Inc.

Stock and Other Ownership Interests: F. Hoffmann-La Roche

Radwa Sharaf

Employment: Foundation Medicine

Stock and Other Ownership Interests: Roche

Brennan Decker

Stock and Other Ownership Interests: Avidea Technologies

Consulting or Advisory Role: Foundation Medicine, Avidea Technologies

REFERENCES

1. Roberts ME, Aynardi JT, Chu CS: Uterine leiomyosarcoma: A review of the literature and update on management options. *Gynecol Oncol* 151:562-572, 2018
2. Seagle BLL, Sobocki-Rausch J, Strohl AE, et al: Prognosis and treatment of uterine leiomyosarcoma: A National Cancer Database study. *Gynecol Oncol* 145:61-70, 2017
3. Horn LC, Schmidt D, Fathke C, et al: New FIGO staging for uterine sarcomas [in German]. *Pathologe* 30:302-303, 2009
4. Amin MB: *AJCC Cancer Staging System*, Eighth Edition. New York, NY, American Joint Committee on Cancer, 2017.

Meagan Montesion

Stock and Other Ownership Interests: Roche

Ethan S. Sokol

Employment: Foundation Medicine

Stock and Other Ownership Interests: Roche (Parent of FMI)

Dean C. Pavlick

Stock and Other Ownership Interests: Roche

Nikunj Shah

Employment: Foundation Medicine

Kevin Jon Williams

Stock and Other Ownership Interests: Hygieia, Gemphire Therapeutics

Consulting or Advisory Role: Gemphire Therapeutics

Research Funding: Novo Nordisk

Jeffrey M. Venstrom

Employment: Genentech, Foundation Medicine

Leadership: Genentech

Stock and Other Ownership Interests: Genentech

Research Funding: Genentech, Roche, Foundation Medicine

Travel, Accommodations, Expenses: Genentech

Brian M. Alexander

Employment: Foundation Medicine

Leadership: Foundation Medicine

Stock and Other Ownership Interests: Roche

Research Funding: Eli Lilly (Inst), Puma (Inst), Celgene (Inst)

(OPTIONAL) Open Payments Link: <https://openpaymentsdata.cms.gov/physician/854258/summary>

Jeffrey S. Ross

Employment: Foundation Medicine

Leadership: Foundation Medicine

Stock and Other Ownership Interests: Foundation Medicine

Consulting or Advisory Role: Celsius Therapeutics

Research Funding: Foundation Medicine

Lee A. Albacker

Employment: Foundation Medicine

Stock and Other Ownership Interests: Roche

Douglas I. Lin

Employment: Foundation Medicine

Shakti H. Ramkissoon

Employment: Foundation Medicine

Stock and Other Ownership Interests: Foundation Medicine

Julia A. Elvin

Employment: Foundation Medicine

No other potential conflicts of interest were reported.

ACKNOWLEDGMENT

We thank the American Association for Cancer Research and appreciate its financial and material support in the development of the American Association for Cancer Research Project GENIE registry, and we thank members of the consortium for their commitment to data sharing.

5. Wang Z, Shi N, Naing A, et al: Survival of patients with metastatic leiomyosarcoma: The MD Anderson Clinical Center for targeted therapy experience. *Cancer Med* 5:3437-3444, 2016
6. Chudasama P, Mughal SS, Sanders MA, et al: Integrative genomic and transcriptomic analysis of leiomyosarcoma. *Nat Commun* 9:144, 2018
7. Yang J, Du X, Chen K, et al: Genetic aberrations in soft tissue leiomyosarcoma. *Cancer Lett* 275:1-8, 2009
8. Moore KN, Gunderson C, Ramkissoon S, et al: Comprehensive genomic profiling of uterine leiomyosarcomas identifies opportunities for personalized therapies. *Ann Oncol* 27:vi309, 2016
9. Davis LE, Nusser KD, Przybyl J, et al: Discovery and characterization of recurrent, targetable *ALK* fusions in leiomyosarcoma. *Mol Cancer Res* 17:676-685, 2019
10. Elvin JA, Gay LM, Ort R, et al: Clinical benefit in response to palbociclib treatment in refractory uterine leiomyosarcomas with a common *CDKN2A* alteration. *Oncologist* 22:416-421, 2017
11. Frampton GM, Fichtenholtz A, Otto GA, et al: Development and validation of a clinical cancer genomic profiling test based on massively parallel DNA sequencing. *Nat Biotechnol* 31:1023-1031, 2013
12. He J, Abdel-Wahab O, Nahas MK, et al: Integrated genomic DNA/RNA profiling of hematologic malignancies in the clinical setting. *Blood* 127:3004-3014, 2016
13. Sun JX, He Y, Sanford E, et al: A computational approach to distinguish somatic vs. germline origin of genomic alterations from deep sequencing of cancer specimens without a matched normal. *PLOS Comput Biol* 14:e1005965, 2018
14. Chalmers ZR, Connelly CF, Fabrizio D, et al: Analysis of 100,000 human cancer genomes reveals the landscape of tumor mutational burden. *Genome Med* 9:34, 2017
15. Trabucco SE, Gowen K, Maund SL, et al: A novel next-generation sequencing approach to detecting microsatellite instability and pan-tumor characterization of 1000 microsatellite instability-high cases in 67,000 patient samples. *J Mol Diagn* 21:1053-1066, 2019
16. Prat J: FIGO staging for uterine sarcomas. *Int J Gynecol Obstet* 104:177-178, 2009
17. Abeshouse A, Adebamowo C, Adebamowo SN, et al: Comprehensive and integrated genomic characterization of adult soft tissue sarcomas. *Cell* 171:950-965.e28, 2017
18. Sweeney SM, Cerami E, Baras A, et al: AACR project GENIE: Powering precision medicine through an international consortium. *Cancer Discov* 7:818-831, 2017
19. Guan KL, Jenkins CW, Li Y, et al: Growth suppression by p18, a p16INK4/MTS1- and p14INK4B/MTS2-related CDK6 inhibitor, correlates with wild-type pRb function. *Genes Dev* 8:2939-2952, 1994
20. Jeffrey PD, Tong L, Pavletich NP: Structural basis of inhibition of CDK-cyclin complexes by INK4 inhibitors. *Genes Dev* 14:3115-3125, 2000
21. Zhu S, Cao J, Sun H, et al: p18 inhibits reprogramming through inactivation of Cdk4/6. *Sci Rep* 6:31085, 2016
22. Park BJ, Kang JW, Lee SW, et al: The haploinsufficient tumor suppressor p18 upregulates p53 via interactions with ATM/ATR. *Cell* 120:209-221, 2005
23. Kim KJ, Park MC, Choi SJ, et al: Determination of three-dimensional structure and residues of the novel tumor suppressor AIMP3/p18 required for the interaction with ATM. *J Biol Chem* 283:14032-14040, 2008
24. Leone PE, Walker BA, Jenner MW, et al: Deletions of *CDKN2C* in multiple myeloma: Biological and clinical implications. *Clin Cancer Res* 14:6033-6041, 2008
25. Kirsch M, Mörz M, Pinzer T, et al: Frequent loss of the *CDKN2C* (p18INK4c) gene product in pituitary adenomas. *Genes Chromosom Cancer* 48:143-154, 2009
26. Grubbs EG, Williams MD, Scheet P, et al: Role of *CDKN2C* copy number in sporadic medullary thyroid carcinoma. *Thyroid* 26:1553-1562, 2016
27. Pohl U, Cairncross JG, Louis DN: Homozygous deletions of the *CDKN2C/p18INK4C* gene on the short arm of chromosome 1 in anaplastic oligodendrogliomas. *Brain Pathol* 9:639-643, 1999
28. Husemann K, Wolter M, Büschges R, et al: Identification of two distinct deleted regions on the short arm of chromosome 1 and rare mutation of the *CDKN2C* gene from 1p32 in oligodendroglial tumors. *J Neuropathol Exp Neurol* 58:1041-1050, 1999
29. Menges CW, Altomare DA, Testa JR: FAS-associated factor 1 (FAF1): Diverse functions and implications for oncogenesis. *Cell Cycle* 8:2528-2534, 2009
30. Jiménez G, Shvartsman SY, Paroush Z: The Capicua repressor: A general sensor of RTK signaling in development and disease. *J Cell Sci* 125:1383-1391, 2012
31. Bettgeowda C, Agrawal N, Jiao Y, et al: Mutations in *CIC* and *FUBP1* contribute to human oligodendroglioma. *Science* 333:1453-1455, 2011
32. Brat DJ, Verhaak RGW, Aldape KD, et al: Comprehensive, integrative genomic analysis of diffuse lower-grade gliomas. *N Engl J Med* 372:2481-2498, 2015
33. Louis DN, Perry A, Reifenberger G, et al: The 2016 World Health Organization Classification of Tumors of the Central Nervous System: A summary. *Acta Neuropathol* 131:803-820, 2016
34. Reifenberger J, Reifenberger G, Liu L, et al: Molecular genetic analysis of oligodendroglial tumors shows preferential allelic deletions on 19q and 1p. *Am J Pathol* 145:1175-1190, 1994
35. Kraus JA, Koopmann J, Kaskel P, et al: Shared allelic losses on chromosomes 1p and 19q suggest a common origin of oligodendroglioma and oligoastrocytoma. *J Neuropathol Exp Neurol* 54:91-95, 1995
36. Cairncross JG, Ueki K, Zlatescu MC, et al: Specific genetic predictors of chemotherapeutic response and survival in patients with anaplastic oligodendrogliomas. *J Natl Cancer Inst* 90:1473-1479, 1998
37. Ohgaki H, Kleihues P: Population-based studies on incidence, survival rates, and genetic alterations in astrocytic and oligodendroglial gliomas. *J Neuropathol Exp Neurol* 64:479-489, 2005
38. Taal W, van der Rijt CCD, Dinjens WNM, et al: Treatment of large low-grade oligodendroglial tumors with upfront procarbazine, lomustine, and vincristine chemotherapy with long follow-up: A retrospective cohort study with growth kinetics. *J Neurooncol* 121:365-372, 2015
39. Griffin CA, Burger P, Morsberger L, et al: Identification of der(1;19)(q10;p10) in five oligodendrogliomas suggests mechanism of concurrent 1p and 19q loss. *J Neuropathol Exp Neurol* 65:988-994, 2006
40. Jenkins RB, Blair H, Ballman KV, et al: A t(1;19)(q10;p10) mediates the combined deletions of 1p and 19q and predicts a better prognosis of patients with oligodendroglioma. *Cancer Res* 66:9852-9861, 2006
41. Horbinski C: Something old and something new about molecular diagnostics in gliomas. *Surg Pathol Clin* 5:919-939, 2012
42. Shoji T, Saito R, Kanamori M, et al: Sarcoma-like tumor originating from oligodendroglioma. *Brain Tumor Pathol* 33:255-260, 2016
43. Rodriguez FJ, Scheithauer BW, Jenkins R, et al: Gliosarcoma arising in oligodendroglial tumors ("oligosarcoma"): A clinicopathologic study. *Am J Surg Pathol* 31:351-362, 2007
44. Hiniker A, Hagenkord JM, Powers MP, et al: Gliosarcoma arising from an oligodendroglioma (oligosarcoma). *Clin Neuropathol* 32:165-170, 2013
45. Mandahl N, Fletcher CDM, Dal Cin P, et al: Comparative cytogenetic study of spindle cell and pleomorphic leiomyosarcomas of soft tissues: A report from the CHAMP Study Group. *Cancer Genet Cytogenet* 116:66-73, 2000
46. Christacos NC, Quade BJ, Dal Cin P, et al: Uterine leiomyomata with deletions of 1p represent a distinct cytogenetic subgroup associated with unusual histologic features. *Genes Chromosom Cancer* 45:304-312, 2006

47. Hodge JC, Pearce KE, Clayton AC, et al: Uterine cellular leiomyomata with chromosome 1p deletions represent a distinct entity. *Am J Obstet Gynecol* 210:P572.E1-572.E7, 2014
48. Nucci MR, Drapkin R, Dal Cin P, et al: Distinctive cytogenetic profile in benign metastasizing leiomyoma: Pathogenetic implications. *Am J Surg Pathol* 31:737-743, 2007
49. Raposo MI, Meireles C, Cardoso M, et al: Benign metastasizing leiomyoma of the uterus: Rare manifestation of a frequent pathology. *Case Rep Obstet Gynecol* 2018:5067276, 2018
50. Bowen JM, Cates JM, Kash S, et al: Genomic imbalances in benign metastasizing leiomyoma: Characterization by conventional karyotypic, fluorescence in situ hybridization, and whole genome SNP array analysis. *Cancer Genet* 205:249-254, 2012
51. Mehine M, Kaasinen E, Mäkinen N, et al: Characterization of uterine leiomyomas by whole-genome sequencing. *N Engl J Med* 369:43-53, 2013
52. Karaskos C, Pandis N, Bardi G, et al: Cytogenetic findings in uterine epithelioid leiomyomas. *Cancer Genet Cytogenet* 80:103-106, 1995
53. Holzmann C, Markowski DN, Koczan D, et al: Genome-wide acquired uniparental disomy as well as chromosomal gains and losses in a uterine epithelioid leiomyoma. *Mol Cytogenet* 7:19, 2014
54. Reyes C, Karamurzin Y, Frizzell N, et al: Uterine smooth muscle tumors with features suggesting fumarate hydratase aberration: Detailed morphologic analysis and correlation with S-(2-succino)-cysteine immunohistochemistry. *Mod Pathol* 27:1020-1027, 2014
55. Arias-Stella JA III, Benayed R, Oliva E, et al: Novel *PLAG1* gene rearrangement distinguishes a subset of uterine myxoid leiomyosarcoma from other uterine myxoid mesenchymal tumors. *Am J Surg Pathol* 43:382-388, 2019
56. Chiang S, Samore W, Zhang L, et al: PGR gene fusions identify a molecular subset of uterine epithelioid leiomyosarcoma with rhabdoid features. *Am J Surg Pathol* 43:810-818, 2019
57. Lee CH, Turbin DA, Sung YCV, et al: A panel of antibodies to determine site of origin and malignancy in smooth muscle tumors. *Mod Pathol* 22:1519-1531, 2009
58. Solomon DA, Kim JS, Jenkins S, et al: Identification of p18 INK4c as a tumor suppressor gene in glioblastoma multiforme. *Cancer Res* 68:2564-2569, 2008
59. Tanboon J, Williams EA, Louis DN: The diagnostic use of immunohistochemical surrogates for signature molecular genetic alterations in gliomas. *J Neuropathol Exp Neurol* 75:4-18, 2016
60. Guo X, Jo VY, Mills AM, et al: Clinically relevant molecular subtypes in leiomyosarcoma. *Clin Cancer Res* 21:3501-3511, 2015



APPENDIX

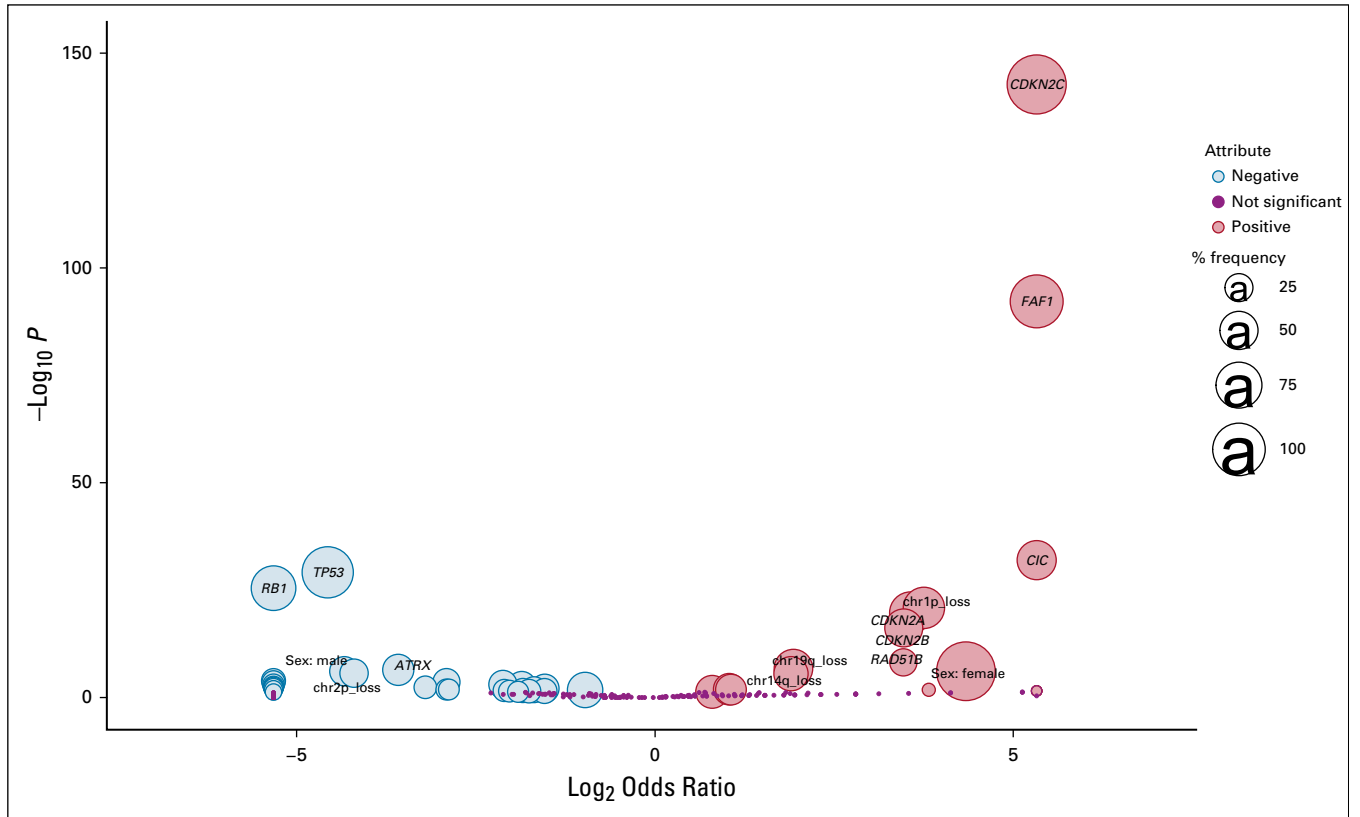


FIG A1. Volcano plot for *CDKN2C*-null leiomyosarcoma. Attributes with *P* value < .0001 are labeled. Red and blue indicate positive and negative correlation, respectively, in *CDKN2C*-null leiomyosarcoma (*n* = 77) compared with the remainder of the leiomyosarcoma cohort (*n* = 2,493). Chromosomal arm-level aneuploidy analysis was available in a subset of *CDKN2C*-null leiomyosarcoma (*n* = 72) and *CDKN2C*-retained leiomyosarcoma (*n* = 1,212).

TABLE A1. List of Sequenced Genes in the FoundationOne CDx and F1H Platforms

Gene Description	ABL1	ACVR1B	AKT1	AKT2	AKT3	ALK	AMER1	APC	AR	ARAF	ARRRP1	ARID1A	ASXL1	ATM	ATR	ATR	ATRX	AURKA	AURKB	AVL	BAP1	
With full coding exonic regions for detection of substitutions, indels, and copy number alterations	BARD1	BCL2	BCL2L1	BCL2L2	BCL6	BCOR	BCORL1	BRAF	BRC1A	BRC2A	BRD4	BRIPI	BTG1	BTG2	BRK	BTIK	BTIK	C11orf50	CALR	CARD11	CBFB	CBL
	CCND1	CCND2	CCNE1	CCNE2	CCNE3	CD70	CD70	CD79A	CD79B	CD79C	CDH1	CDK12	CDK4	CDK6	CDK8	CDKN1A	CDKN1B	CDKN2A	CDKN2B	CDKN2C		
	CEBPA	CHEK1	CHEK2	CIC	CREBBP	CRKL	CSF1R	CSF3R	CTCF	CTNNA1	CTNNB1	CUL3	CXCR4	DAXX	DDR2	DNAH3	DOT1L	EED	EGFR	EP300		
	EPHA3	EPHB1	ERBB2	ERBB3	ERBB4	ERG	ERRF1	ESR1	EZH2	FAM123B	FAM46C	FANCA	FANCC	FANCF	FANCL	FAS	FBXW7	FGF10	FGF14	FGF19		
	FGF23	FGF3	FGF4	FGF6	FGFR1	FGFR2	FGFR3	FGFR4	FH	FLOW	FLT1	FLT3	FOXL2	FUBP1	GABRA6	GATA3	GATA4	GATM6	GID4	GNAI1		
	GNAI3	GNAQ	GNAS	GRM3	GSK3B	H3F3A	HDA1C	HGF	HNF1A	HNRAS	HSD3B1	IGF1R	IDH1	IDH2	IKZF1	IKZF2	IKZF3	IKZF4	IKZF5			
	IRS2	JAK1	JAK2	JAK3	JUN	KOM6A	KOM6C	KOM6A	KOR	KGAP1	KEL	KIT	KLHL6	KMT2A	KMT2D	KRAS	LYN	MAF	MAP2K1	MAP2K2		
	MAP2K4	MAP3K1	MAPK1	MAPK3	MAPK8	MED12	MEF2B	MEN1	MET	MIF	MLH1	MMS1	MMS2	MPL	MRE11A	MSH2	MSH3	MSH4	MSH6	MTAP		
	MTOR	MUTYH	MYC	MYCL	MYCN	MYD88	NF1	NF2	NFE2L2	NFKBIA	NKX2-1	NOTCH1	NOTCH2	NOTCH3	NP1	NRAS	NSD2	NSD3	NTSC2	NTRK1		
	NTRK2	NTRK3	P2RY8	PALB2	PARK2	PAX5	PBRM1	PDCD1	PDCD1LG2	PDGFRA	PDGFRB	PDK1	PKC2CB	PKC3CB	PKG3CB	PKR1	PIM1	PIM2	POLD1	POLE		
	PPP2R1A	PRDM1	PRKCI	PRKN	PTEN	PTPN11	PTPR	PTPRB	PTPRG	QKI	RAC1	RAD21	RAF1	RARA	RBI	RBM10	RET	RNF43				
	ROSI	RPTOR	SDHA	SDHB	SDHC	SETD2	SF3B1	SGK1	SMAD2	SMAD4	SMARCA4	SMARCA4	SMA4	SNAI1	SNAI2	SNAI3	SPO1	SPO2	SPO3			
	SRC	STAG2	STAI3	STK11	SUFU	SYK	TBKG	TERT	TET2	TGFB2	TNFAIP3	TNFRSF14	TP53	TSC1	TSC2	U2AF1	VEGFA	VHL	WHSC1	WHSC1L1		
	WT1	WTX	XPO1	ZNF217	ZNF703																	
With select intronic regions	ALK	BCL2	BCR	BRAF	BRC1A	BRC2A	EGFR	ETV4	ETV5	ETV6	ENSR1	FGFR1	FGFR2	FGFR3	KIT	KMT2A	MSH2	MYB	MYC	NOTCH2		
	NTRK1	NTRK2	NUTM1	PDGFRA	RAF1	RARA	RET	ROSI	SLC34A2	TERT	TPRSS2											
In F1H DNA panel																						
With full coding exonic regions for detection of substitutions, indels, and copy number alterations	AB1	ACTB	ADGR2	AKT1	AKT2	AKT3	ALK	AMER1	APC	APH1A	AR	ARAF	ARRRP1	ARHGAP26	ARID1A	ARID2	ASMTL	ASXL1	ATM	ATR		
	ATRX	AURKA	AURKB	AXIN1	AXL	B2M	BAP1	BARD1	BCL10	BCL11B	BCL2	BCL2L2	BCL6	BCOR	BCORL1	BIRC3	BLM	BRAF	BRC1A	BRC2A		
	BRD4	BRIPI	BRSK1	BTG1	BTG2	BTY	BTLA	BTNA1	C17orf39	CAD	CARD11	CBFB	CBL	CCND1	CCND2	CCND3	CCNE1	CCTEB	CCZ2	CD274		
	CD36	CD58	CD70	CD79A	CD79B	CD79C	CDH1	CDK1	CDK4	CDK6	CDK8	CDKN1B	CDKN2A	CDKN2C	CDKN3	CEBPA	CHEK1	CHEK2	CIC	CIITA		
	CXSB1	CP1	CREBBP	CRKL	CRLF2	CSF1R	CSF3R	CTCF	CTNNA1	CTNNB1	CUX1	CXCR4	DAXX	DDR2	DDX3X	DNM2	DNMT3A	DOT1L	DTX1	DUSP2		
	DUSP9	E2F1	E2F2	E2F3	E2F4	E2F5	ELP2	EMSY	EP300	EPHA3	EPHA4	EPHA7	EPH2	EPH3	ERBB2	ERBB3	ERBB4	ERG	ESR1	ETS1		
	ETV6	EXOSC6	EZH2	F1	F1L1	F1L2	F1L3	F1L4	F1L5	F1L6	F1L7	F1L8	F1L9	F1L10	F1L11	F1L12	F1L13	F1L14	F1L15	F1L16	F1L17	F1L18
	FGF23	FGF3	FGF4	FGF6	FGFR1	FGFR2	FGFR3	FGFR4	FHIT	FLOW	FLT1	FLT3	FLT4	FLYWCH1	FOXO1	FOXO3	FOXO4	FOXO6	FOXO7	FOXO8	FOXO9	FOXO9
	GATA1	GATA2	GATA3	GID4	GNAI1	GNAI2	GNAI3	GNAQ	GNAS	GRI24	GRAF	GRIN2A	GSK3B	GSEI	HDAC1	HDAC4	HDAC7	HGF	HIST1H1C	HIST1H1D		
	HIST1H1E	HIST1H2AC	HIST1H2AG	HIST1H2AL	HIST1H2AM	HIST1H2BC	HIST1H2BD	HIST1H2BE	HIST1H2BF	HIST1H2BG	HIST1H2BI	HIST1H2BJ	HIST1H2BK	HIST1H2BL	HIST1H2BM	HIST1H2BN	HIST1H2BO	HIST1H2BP	HIST1H2BQ	HIST1H2BR	HIST1H2BS	HIST1H2BT
	IKZF3	IL7R	INHA	INPP4B	INPP5D	IRF1	IRF4	IRF8	IRS2	JAK1	JAK2	JAK3	JARID2	JUN	KAT5A	KOM2B	KOM4C	KOM6A	KOM6C	KOM6A		
	KDR	KEAP1	KIT	KLHL6	KMT2A	KMT2C	KRAS	LEF1	LMO1	LRRK1	LRRK2	MAF	MAFB	MAGED1	MALTI	MAP2K1	MAP2K2	MAP2K4	MAP3K1	MAP3K14		
	MAP3K6	MAP3K7	MAPK1	MAPK2	MAPK3	MAPK4	MAPK5	MAPK6	MAPK7	MAPK8	MAPK9	MAPK10	MAPK11	MAPK12	MAPK13	MAPK14	MAPK15	MAPK16	MAPK17	MAPK18	MAPK19	MAPK20
	MRE11A	MSH2	MSH3	MSH4	MSH6	MTOR	MUTYH	MYC	MYCL	MYD88	MPO18A	MYST3	NCOR2	NCOR3	NCOA2	NCOA3	NCOA4	NCOA5	NCOA6	NCOA7	NCOA8	NCOA9
	NOD1	NOTCH1	NOTCH2	NPW1	NRAS	NSD1	NSD2	NTF5C2	NTRK1	NTRK2	NTRK3	NUP93	NUP98	P2RY8	PAG1	PAK3	PALB2	PASK	PAK5	PBRM1		
	PC	PCBP1	PCLO	PDCD1	PDCD1L	PDCD1LG2	PDGFRA	PDGFRB	PDK1	PDLL1	PDLL2	PHF6	PIK3CA	PIK3CG	PIK3R1	PIK3R2	PIK3R3	POT1	POLR2A	PRDM1		
	PRKARIA	PRKDC	PRSS8	PST1	PST2	PST3	PST4	PST5	PST6	PST7	PST8	PST9	PST10	PST11	PST12	PST13	PST14	PST15	PST16	PST17	PST18	PST19
	RNF43	ROSI	RPTOR	RUNX1	RUNX1T1	SJPR2	SDHA	SDHB	SDHC	SDHD	SENP2	SETBP1	SETD2	SF3B1	SGK1	SHIP	SHIP1	SHIP2	SHIP3	SHIP4	SHIP5	SHIP6
	SMARCA4	SMARCB1	SMG1A	SMG3	SMO	SOC1	SOC2	SOC3	SOX10	SOX2	SPEN	SPOP	SRC	SRSF2	STAT2	STAT3	STAT4	STAT5A	STAT5B	STAT6	STAT7	STAT8
	STK11	SUFU	SUZ12	SYK	TAF1	TBL1XR1	TGFB2	TGFB3	TGFB4	TGFB5	TGFB6	TGFB7	TGFB8	TGFB9	TGFB10	TGFB11	TGFB12	TGFB13	TGFB14	TGFB15	TGFB16	TGFB17
	TOP1	TP53	TP63	TRAF2	TRAF3	TRAF5	TSC1	TSC2	TUSC3	TYK2	U2AF1	U2AF2	VHL	WDR90	WHSC1	WIP1	WT1	WTX	XBPI	XPO1		
	YY1AP1	ZMYM2	ZNF217	ZNF24	ZNF703	ZRSR2	ZSCAN3															
With select intronic regions	ALK	BCL2	BCL6	BCR	BRAF	CCND1	CRLF2	EGFR	EPOR	ETV4	ETV5	ETV6	ENSR1	FGFR2	IGH	IGK	IGL	JAK1	JAK2			
	KMT2A	MLL	MYC	NTRK1	PDGFRA	PDGFRA	RAF1	RARA	RET	ROSI	TPRSS2	TRG										

TABLE A2. Locations of Sequenced Tumor Specimens

Location	No. of Cases
Primary site	29
Uterine	25
Abdominal wall	1
Hip/gluteal	1
Sacrum	1
Small bowel	1
Metastatic site	48
Lung	7
Retroperitoneum	5
Abdominal wall	4
Limb soft tissue	4
Omentum	4
Liver	3
Paraspinal	3
Peritoneum	3
Pleura	2
Colon	2
Kidney	2
Chest wall	2
Mesentery	2
Small intestine	1
Hilar lymph node	1
Vagina	1
Posterior mediastinum	1
Heart	1

TABLE A3. Comparisons of the Frequencies of Genomic Alterations in *CDKN2C*-Null LMS Versus All Non-*CDKN2C*-Null LMS Cases, as Well as Non-*CDKN2C*-Null LMS Cases With 19/19Q-Codeletion ^{c/c} Mutation, *CDKN2A*, and *RAD51B* Mutations, or *ALK* Fusion

Variable	LMS Cases Without Homozygous Deletion of <i>CDKN2C</i>						
	<i>CDKN2C</i> -Null LMS	All <i>CDKN2C</i> -Retained LMS	1p/19q-Codeleted LMS	<i>CIC</i> -Mutant LMS	<i>CDKN2A</i> -Mutant LMS	<i>RAD51B</i> -Mutant LMS	<i>ALK</i> -Rearranged LMS
No. of patient cases	77	2,493	62	35	175	43	41
Female sex, % (n/total N)	99 (76/77)	79 (1,968/2,493)	87 (54/62)	86 (30/35)	83 (146/175)	98 (42/43)	98 (40/41)
Median (range) age, years	61 (36-81)	57 (< 1 to ≥ 89)	56 (33-78)	57 (34-81)	59 (< 1-86)	57 (37-80)	58 (17-75)
Median (Q1-Q3) TMB, mut/Mb	2.4 (1.6-3.2)	2.4 (1.6-4.0)	2.5 (1.6-5.0)	2.4 (1.6-4.2)	3.2 (2.4-4.0)	3.8 (2.0-5.0)	3.2 (1.6-4.0)
MSI high	0 (0/63)	0.2 (5/2,093)	2 (1/62)	0 (0/30)	1 (1/146)	0 (0/37)	0 (0/35)
Genomic alteration, % (n/total N)							
<i>TP53</i>	12 (9/77)	73 (1,830/2,493)	52 (33/62)	51 (18/35)	46 (80/175)	70 (30/43)	37 (15/41)
<i>RBI</i>	0 (0/77)	55 (1,359/2,493)	45 (28/62)	49 (17/35)	14 (25/175)	63 (27/43)	15 (6/41)
<i>ATRX</i>	3 (2/77)	25 (606/2,473)	16 (10/62)	17 (6/35)	12 (20/172)	30 (13/43)	5 (2/40)
<i>PTEN</i>	9 (7/77)	16 (399/2,493)	13 (8/62)	17 (6/35)	9 (15/175)	19 (8/43)	5 (2/41)
1p/19q-codeletion	81 (58/72)	5 (62/1,212)	100 (62/62)	22 (4/18)	17 (14/82)	19 (5/26)	32 (6/19)
<i>CIC</i>	40 (31/77)	1 (35/2,473)	7 (4/62)	100 (35/35)	0 (0/172)	9 (4/43)	0 (0/40)
<i>CDKN2A</i>	47 (36/77)	7 (175/2,493)	23 (14/62)	0 (0/35)	100 (175/175)	5 (2/43)	63 (26/41)
<i>RAD51B</i>	17 (13/77)	2 (43/2,473)	8 (5/62)	11 (4/35)	1 (2/172)	100 (43/43)	5 (2/40)
<i>ALK</i> fusion	3 (2/77)	2 (41/2,493)	10 (6/62)	0 (0/35)	15 (26/175)	5 (2/43)	100 (41/41)
<i>BRAF</i> fusion	3 (2/77)	0.2 (4/2,493)	0 (0/62)	0 (0/35)	0 (0/175)	2 (1/43)	0 (0/41)
<i>FGFR1</i> fusion	1 (1/77)	0.1 (2/2,493)	0 (0/62)	0 (0/35)	0 (0/175)	0 (0/43)	0 (0/41)
<i>NTRK1</i> fusion	1 (1/77)	0.1 (3/2,493)	0 (0/62)	0 (0/35)	1 (2/175)	0 (0/43)	0 (0/41)

NOTE. For percent values, the number of positive cases over the number of evaluated cases is included in parentheses. Abbreviations: LMS, leiomyosarcoma; MSI, microsatellite instability; TMB, tumor mutational burden.

TABLE A4. Results With Available Paired Specimens

Patient	Initial Results		Paired Specimen Results		Time to Paired Specimen
	Specimen Site	Sequencing Results	Specimen Site	Sequencing Results	
1	Primary uterine	TP53 p.R342*, homozygous loss of CDKN2C	Right lung mass	TP53 p.R342*, homozygous loss of CDKN2C , <i>FAFI</i> exon 1-2, <i>CIC</i> exon 1, and <i>RB1</i> exon 9-17	13 months
2	Ileum (from uterine primary)	Homozygous loss of CDKN2C , FAFI , CDKN2A , CDKN2B , and TP53	Peritoneal mass	Homozygous loss of CDKN2C , FAFI , CDKN2A , CDKN2B , TP53 , <i>FAS</i> , and <i>FANCA</i> . <i>FANCD2-EMC3</i> rearrangement exon 34	27 months
3	Retroperitoneal mass (indeterminant primary)	Homozygous loss of CDKN2C	Abdominal wall	Homozygous loss of CDKN2C	22 months

NOTE. Matching genomic alterations are in bold.